

Microporous Materials of Metal Carboxylates

Wasuke Mori^{*,1} and Satoshi Takamizawa^{*†}

^{*}Department of Chemistry, Faculty of Science, Kanagawa University, Hiratsuka, Kanagawa 259-1293, Japan; and

[†]Department of Chemistry, Graduate School of Science, Osaka University, Toyonaka, Osaka 560-0043, Japan

Copper(II) terephthalate absorbs a large amount of gases such as N₂, Ar, O₂, and Xe. The maximum amounts of absorption of gases were 1.8, 1.9, 2.2, and 0.9 mole per mole of the copper(II) salt for N₂, Ar, O₂, and Xe, respectively, indicating that the gases were not adsorbed on the surface but occluded within the solid. Other microporous copper(II) dicarboxylates are also reviewed. The porous structure of copper(II) terephthalate, in which the gas is occluded, is deduced from the temperature dependence of magnetic susceptibilities and the linear structure of terephthalate. Microporous molybdenum(II) and ruthenium(II, III) dicarboxylates are discussed. We describe that rhodium(II) monocarboxylate bridged by pyrazine form stable micropores by self-assembly of infinite linear chain complexes. © 2000 Academic Press

1. INTRODUCTION

The mineral zeolite was reported by Cronstedt in 1756 and Damour in 1840 (1). In the 20th century, numerous porous compounds (either natural or artificial) became recognized. Zeolite, porous silica, Cray, activated carbon, fabric carbon, etc., are well known classical porous materials (2). They are classified by their components (organic and inorganic), the degree of crystallization, pore-size, and functions.

In the middle of the 20th century, study of the magnetic behavior of copper(II) acetate derivatives (3) which have the well-known dimer structure (4), became quite popular. Mori, one of the authors of this paper, prepared the copper(II) terephthalate as microcrystals for investigating magnetic interaction of interdimer. When we were measuring the temperature dependencies of the magnetic susceptibility of copper(II) terephthalate by a Faraday balance with a Cahn electric balance under a nitrogen atmosphere, we found incidentally that a large amount of N₂ gas was occluded in the copper(II) salt. It was confirmed by anomalous increase

of weight at low temperature (5). Figure 1 shows the Faraday magnetometer.

The temperature dependence of the magnetic susceptibilities of copper(II) terephthalate, as shown in Fig. 2, obeyed the Bleaney–Bowers equation (6) for $S = 1/2$ Heisenberg model of dimer structure observed in many copper(II) complexes (7) forming the same dinuclear structure as copper(II) acetate (8). It is reasonable to assume that the copper(II) terephthalate comprises the same configuration as the copper(II) acetate monohydrate, so that considering the linear structure of terephthalate, two-dimensional lattice structure is proposed for copper(II) terephthalate (9) (see Fig. 3). The temperature dependence of the amount of absorbed gases were gravimetrically measured by a Cahn 1000 electric balance. The amounts of absorbed N₂, Ar, and O₂ were almost completely saturated at the temperature of liquid nitrogen as shown in Fig. 4. The amount of adsorbed gas is enormous. For example, over 30 g (30 L) of O₂ was absorbed in the 100 g of copper(II) terephthalate. The pore size was calculated by the Horvath–Kawazoe equation (10) from the absorption isotherm of copper(II) terephthalate at the temperature of liquid argon. The shape of isotherm was Type I according the IUPAC classification (11). A very narrow peak at ca. 6 Å suggests that regular and stable ultramicropores are constructed by copper(II) terephthalate in a solid state (see Fig. 5).

In this paper we report on the syntheses and gas occlusion properties of the microporous complexes of metal carboxylates.

On the isomorphous zinc(II) terephthalate, the research has been made by Yaghi (12).

2. DESIGN STRATEGY TO SYNTHESIZE MICROPOROUS COMPLEXES

Because we found that copper(II) terephthalate occluded large amounts of nitrogen gas, several transition-metal dicarboxylates were synthesized as the first step in making new porous materials. Polydentate ligands are suitable for constructing stable covalent networks: the softness of the

¹To whom correspondence should be addressed. E-mail: wmori@info.kanagawa-u.ac.jp.

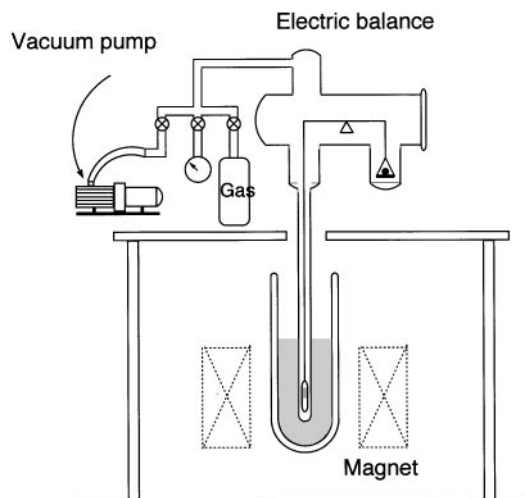


FIG. 1. Magnetic balance.

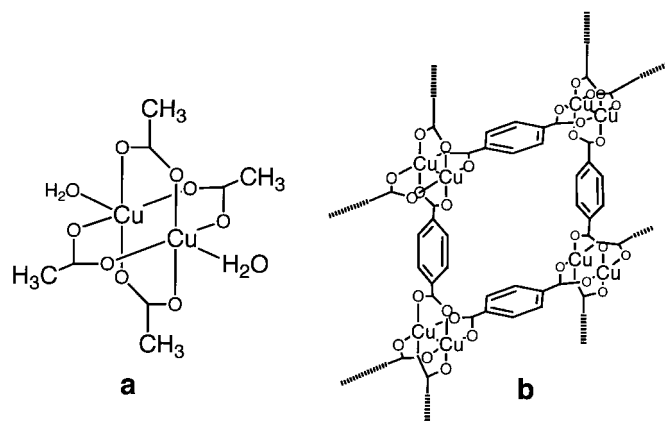


FIG. 3. Molecular structure of copper(II) acetate monohydrate (a) and the deduced two-dimensional structure of copper(II) terephthalate (2) and its micropore (b).

structure will be required. The use of molecular assembly is also favored to produce porous complexes in a solid state. The general method to synthesizing a 3D porous complex is drawn in Fig. 6. The intermolecular interactions in constructing the porous structure composed of lower dimensional building blocks. In this study, we selected dinuclear carboxylates as the building blocks.

Dinuclear metal carboxylates, $M_2(O_2CR)_4$, represent an important class of transition metal complexes with respect to the study of metal-metal interaction. The most representative series is the carboxylates for $M = Cr^{13}$, Mo^{14} , W^{15} , Re^{16} , Ru^{17} . They are represented by the general formula $M_2(O_2CR)_4L_2$ and have a lantern-like structure, as shown in Fig. 7a. Dinuclear complexes bearing metal-metal bonds have been synthesized and characterized crystallographi-

cally, and the nature of their multiple bonds has been theoretically and spectroscopically investigated. They are reviewed by Cotton and Walton (18).

Generally, a two- or three-dimensional network is built up of bridges of dicarboxylate or polycarboxylate ligands (19). In the case of the linear dicarboxylate bridge, it is obvious that two-dimensional lattices are constructed, and infinite linear micropores are created by stacking the two-dimensional lattices as shown in Fig. 7b and 7c.

2.1. Metal Dicarboxylate

Copper(II) dicarboxylates. Copper(II) terephthalate (2) is the first transition-metal complex capable of adsorbing gases reversibly. This complex has opened a new area of

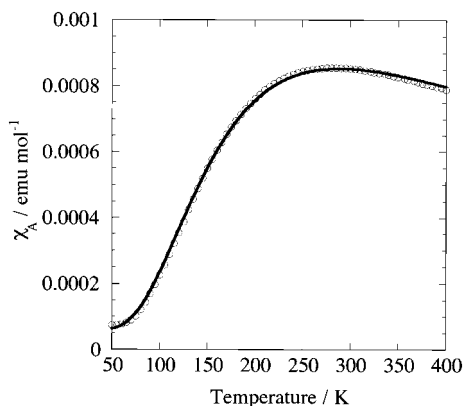


FIG. 2. Temperature dependence of magnetic susceptibilities of copper(II) terephthalate (2). The solid line is the best-fit curve of the Bleaney-Bowers equation with $2J = -321 \text{ cm}^{-1}$, $g = 2.20$, and $N\alpha = 60 \times 10^{-6} \text{ emu mol}^{-1}$.

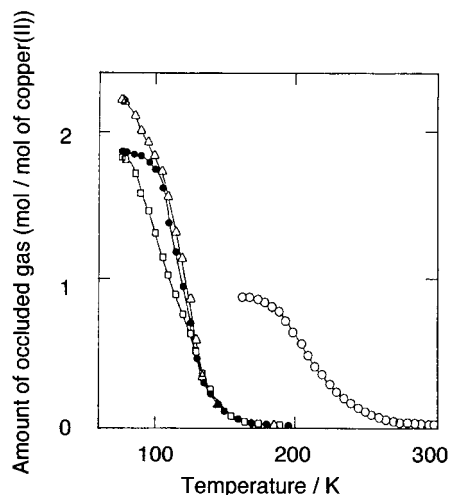


FIG. 4. Isobar of copper(II) terephthalate (2) for N_2 (□), Ar (●), O_2 (Δ), and Xe (○) at 20 Torr.

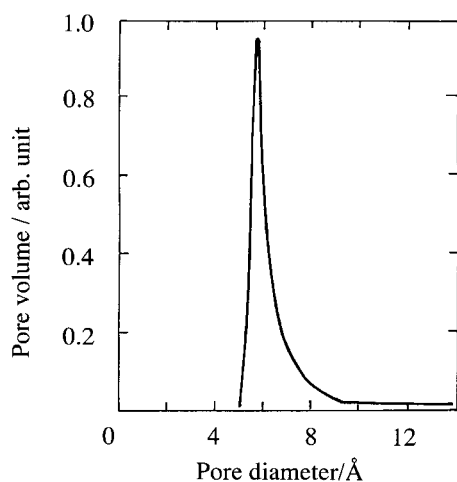


FIG. 5. Pore diameter of copper(II) terephthalate (2).

complex chemistry and has become recognized as a principal complex in the construction of microporous complexes. This copper(II) salt forms during the reaction of copper(II) formate with terephthalic acid in methanol in the presence of formic acid. After standing several weeks in a moisture-free environment, the blue plates were precipitated (Scheme 1). Heating the crystals for 2 h at 110°C in a vacuum, produced greenish blue microcrystals, which are capable of absorbing gases. The greenish blue microcrystals show very sharp powder X-ray diffraction, indicating that the adsorbent consists of a rigid crystalline material. The other copper(II) dicarboxylates were synthesized in a similar manner.

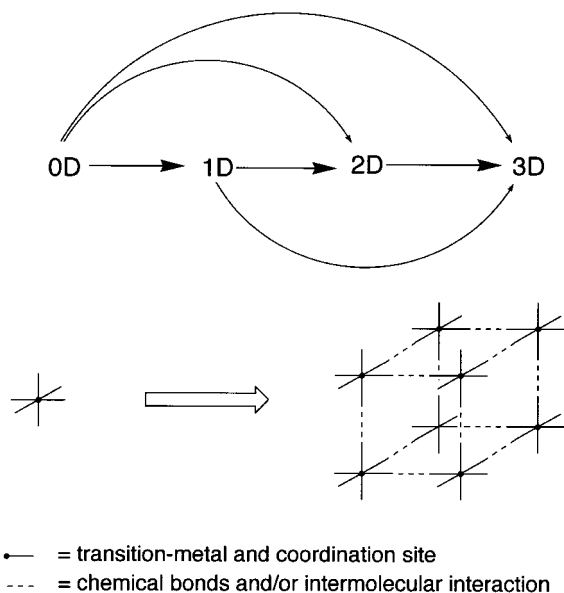


FIG. 6. Three-dimensional lattice organized by the assembly of lower dimensional building blocks.

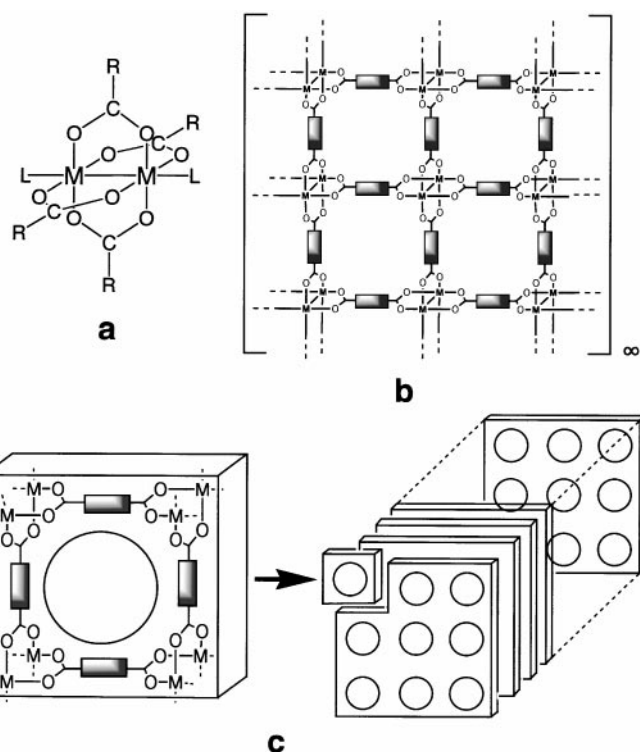
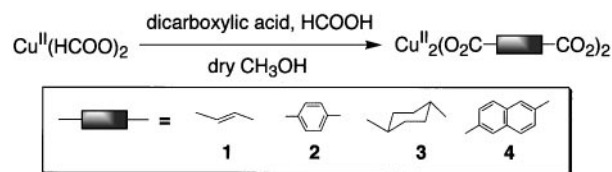


FIG. 7. Lantern-like structure (a), two-dimensional lattice structure (b), and porous structure (c).

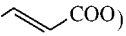
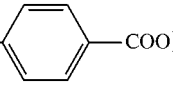
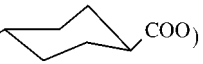
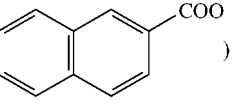
Several copper(II) dicarboxylates (20) (fumarate (1), 2,6-naphthalenedicarboxylate (3), and *trans*-1,4-cyclohexanedicarboxylate (4)) capable of adsorbing gases such as N₂, O₂, Ar, and CH₄ are obtained. Those complexes reversibly adsorb gases without any structural damages. The amounts of gas adsorbed and the pore sizes of the copper complexes are summarized in Table 1. The pore sizes of copper(II) dicarboxylates are controllable by the size and structure of dicarboxylate ligands.

Molybdenum(II) dicarboxylates (21). Molybdenum(II) dicarboxylates are successfully obtained by a ligand exchange reaction of acetate (22) in dry methanol media under an argon atmosphere (Scheme 2). Molybdenum(II) dicarboxylates (5–9) are obtained as an insoluble powder. The bands in the Raman and infrared spectra of 5–9 are sum-



SCHEME 1

TABLE 1
Adsorbent Properties of Copper(II) Dicarboxylates 1–4

Copper(II) dicarboxylate		Amount of occluded N ₂ (mol/mol of copper atoms)	Averaged pore diameter ^a (Å)
Cu(OOC-  -COO)	1	0.8	5.4
Cu(OOC-  -COO)	2	1.8	6.0
Cu(OOC-  -COO)	3	1.1	4.9
Cu(OOC-  -COO)	4	1.1	Not measured

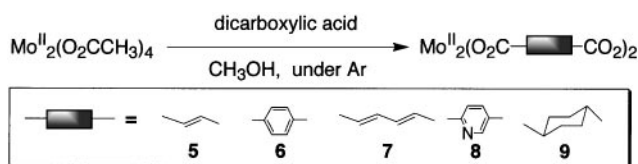
^aHorvath-Kawazoe method.

marized in Table 2. The strongest bands in the Raman spectra of **5–9** occur at 386–398 cm⁻¹ in the solid. These bands are assigned to $\nu(\text{Mo-Mo})$ by comparison with the acetate spectrum in the assignment of the strong band 406 cm⁻¹ to the A_{1g} mode consisting predominantly of Mo-Mo stretching (23). The decrease of about several cm⁻¹ in going from the acetate to **5–9** may indicate a slight weakening of the metal-metal bond. This phenomenon may be due to interdimeric overlap of MOs in the axial direction, but is not due to the effect of π -conjugation in the ligands, because the same decrease is observed in **9**, which has no π -conjugation. Especially in the case of **8**, axial coordination of the pyridine nitrogen in the ligand to molybdenum in the neighboring dinuclear moiety may occur. In the infrared spectra the strongest two bands were observed in the C-O stretching region; they were assigned to the asymmetric and symmetric stretching modes. The infrared spectra are very similar to those of molybdenum(II) acetate (24).

The maximum amounts adsorbed, which were evaluated from the saturated amount with isobars ($p = 20$ Torr), are summarized in Table 3. The maximum amount of adsorbed nitrogen for **2** is 2.0 mol, which is ever so slightly more than that of copper(II) terephthalate. The temperature dependencies of gas adsorption for molybdenum(II) complexes **5–9**

are also very similar to that of copper(II) dicarboxylates, described in the previous section. This similarity of gas-adsorption behavior suggests that molybdenum(II) dicarboxylates **5–9** have the isomorphous structure of copper(II) dicarboxylates.

Solid-state magic angle spinning (MAS) NMR probes the local structure of the host lattice complexes and the environment of the guest molecules. The ¹³C CP/MAS NMR investigation of the complexes was conducted at a spinning speed of 5 kHz at room temperature. The shifts in chemical values observed for **5** through **9** are listed in Table 4. The ¹³C CP/MAS NMR spectra of complex **6** with adsorbed *n*-butane (a) and the dried complex (b) are shown in Fig. 8. Two additional peaks of spectrum (a) corresponding to the methyl and methylene groups of *n*-butane appeared at 24.8 and 13.4 ppm, respectively. The line width of the *n*-butane is small, suggesting rapid motion of *n*-butane molecules adsorbed in complex **6**. Three spectra of **6** for the shift region of the benzene ring (120–140 ppm) are shown in Fig. 9. In the spectrum (a) of the dried **2**, two signals located at 130.1 and 133.0 ppm were clearly assigned to the C₂ and C₁ carbons, respectively, by the use of a dipolar-dephasing spectrum (b) in which the signal of the C₂ carbon bonded to proton nuclei disappeared and the signal of the carbon bonded to the carboxyl group remained. Spectrum (c) shows a significant change in the chemical environment of the C₂ carbon of the phenyl ring of the terephthalate ligand by occluding the *n*-butane molecules in complex **6**. The signal of the C₂ carbon shifts to a lower field by 0.8 ppm, while other signals, including that of carboxyl carbon, remain almost constant. This result shows that the adsorbed molecules apparently interact with C₂ carbons. The line width showed no significant broadening, suggesting a homogeneous change in the environment of the benzene rings of all the



SCHEME 2

TABLE 2
Results from Raman and IR Spectra of Molybdenum(II) Dicarboxylates 5–9

Complex		Raman $\nu_{\text{Mo-Mo}}/\text{cm}^{-1}$	IR	
			$\nu_{\text{asymOCO}}/\text{cm}^{-1}$	$\nu_{\text{symOCO}}/\text{cm}^{-1}$
$\text{Mo}_2(\text{O}_2\text{CCH}_3)_4$		406	1500	1435
$\text{Mo}_2(\text{OOC}-\text{CH}=\text{CH}-\text{COO})_2$	5	398	1498	1397
$\text{Mo}_2(\text{OOC}-\text{C}_6\text{H}_4-\text{COO})_2$	6	399	1506	1387
$\text{Mo}_2(\text{OOC}-\text{CH}=\text{CH}-\text{CH}=\text{CH}-\text{COO})_2$	7	389	1487	1372
$\text{Mo}_2(\text{OOC}-\text{C}_5\text{H}_4\text{N}-\text{COO})_2$	8	386	1523	1397
$\text{Mo}_2(\text{OOC}-\text{C}_{10}\text{H}_{16}-\text{COO})_2$	9	399	1505	1420

terephthalate ligands, which make up the micropores. The change in the local structure of complex **6** due to the adsorption of *n*-butane is reversible. These results strongly indicate that gas molecules are adsorbed homogeneously in micropores surrounded by a quartet of terephthalate ligands.

Ruthenium(II, III) dicarboxylates (25). Since the discovery of binuclear tetra- μ -carboxylates of ruthenium(II,III) $\text{Ru}_2(\text{O}_2\text{CR})_4\text{Cl}$, various studies have prompted much interest in ruthenium(II,III) acetate derivatives in the field of

solid-state physics and chemistry (26) because of their halogen bridged $-\text{Ru}-\text{Ru}-\text{X}-$ mixed-valence structure and the +2.5 oxidation state of the ruthenium atom with a $(\sigma)^2(\pi)^4(\delta)^2(\pi^*)^2(\delta^*)^1$ configuration per dinuclear (27) (see Fig. 10a). We have focused on ruthenium (II,III) dicarboxylate derivatives, which will make up a more rigid network structure, assisted by the axial-halogen bridge, than those of copper(II) dicarboxylates and molybdenum(II) dicarboxylates.

Complexes of $\text{Ru}_2(\text{trans-O}_2\text{C-CH=CH-CO}_2)_2\text{Cl}$ (**10**), $\text{Ru}_2(\text{trans-trans-O}_2\text{C-CH=CH-CH=CH-CO}_2)_2\text{Cl}$ (**11**),

TABLE 3
Amounts of Adsorbed Gases in Molybdenum(II) Dicarboxylates 5–9

Complex		Amount of occlusion (mol/mol of molybdenum(II))			
		N_2	Ar	O_2	CH_4
$\text{Mo}_2(\text{OOC}-\text{CH}=\text{CH}-\text{COO})_2$	5	1.1	1.2	1.4	0.9
$\text{Mo}_2(\text{OOC}-\text{C}_6\text{H}_4-\text{COO})_2$	6	2.0	1.9	2.1	2.0
$\text{Mo}_2(\text{OOC}-\text{CH}=\text{CH}-\text{CH}=\text{CH}-\text{COO})_2$	7	1.0	1.2	1.7	1.2
$\text{Mo}_2(\text{OOC}-\text{C}_5\text{H}_4\text{N}-\text{COO})_2$	8	0.8	1.0	1.2	0.6
$\text{Mo}_2(\text{OOC}-\text{C}_{10}\text{H}_{16}-\text{COO})_2$	9	0.7	0.8	Not measured	Not measured

TABLE 4
Isotropic Chemical Shifts of $^{13}\text{C}/\text{MAS}$ NMR Spectra of 5–9

Complex	$\delta_{\text{iso}}/\text{ppm}$ (assignment)
5	131.0 (ene), 177.0 (carbonyl)
6	130.1, 133.0 (benzene), 176.8 (carbonyl)
7	126.8, 141.8 (diene), 177.1 (carbonyl)
8	127.2, 138.6, 149.9 (pyridine ring), 174.0 (carbonyl)
9	30.2, 42.1, 45.5 (cyclohexane ring), 187.9 (carbonyl)

and $\text{Ru}_2(p\text{-O}_2\text{C-C}_6\text{H}_4\text{-CO}_2)_2\text{Cl}$ (**12**) were synthesized by a ligand exchange method between $\text{Ru}_2(\text{O}_2\text{CCH}_3)_4\text{Cl}$ and appropriate dicarboxylic acids in the presence of lithium chloride. (Scheme 3). A high yield of insoluble brown powder was obtained.

Raman, far-IR, and magnetic measurements revealed that the electronic structures of **10–12** are very similar to that of $\text{Ru}_2(\text{O}_2\text{CCH}_3)_4\text{Cl}$ (**28**), as shown in Table 5. In Raman spectra, $\nu(\text{Ru-Ru})$ occurs at around 330 cm^{-1} . In far-IR spectra, bands are observed in two regions at around 400 and 340 cm^{-1} , which are assigned to Ru-O and Ru-Cl stretching modes, respectively (29). Raman and far-infrared spectra indicate that these compounds have a dinuclear structure that combines with the halide ion at the axial coordination site. The effective magnetic moments at room temperature are in the range 3.75 and 4.04 BM per dinuclear, consistent with the values obtained previously for Ru(II)-Ru(III) compounds and species containing three unpaired electrons per dinuclear with the ground electronic configuration of $(\sigma)^2(\pi)^4(\delta)^2(\pi^*)^2(\delta^*)^1$. In view of their similarity to mixed-valence $\text{Ru}_2(\text{O}_2\text{CR})_4\text{Cl}$ derivatives, it is most likely that the chloride anions in **10–12** link two

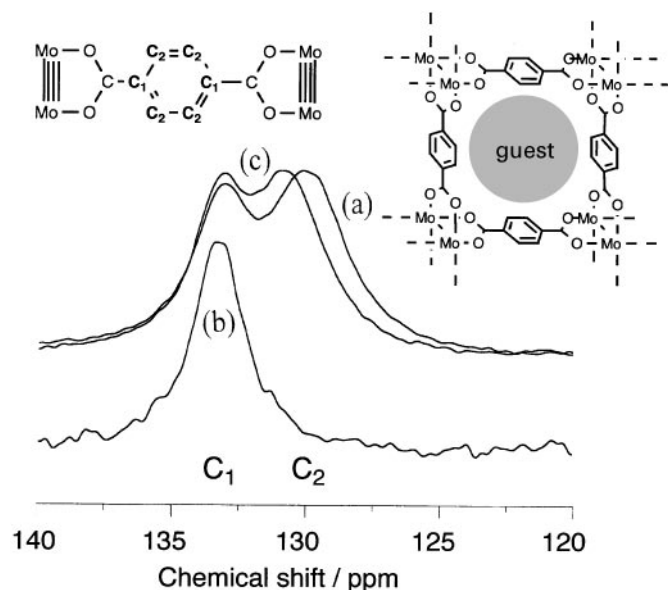


FIG. 9. ^{13}C CP/MAS NMR spectra of **6** magnified in the shift of the benzene region; (a) **2**, (b) dipolar dephased spectrum of **6**, (c) **6** occluding *n*-butane.

ruthenium ions to construct linear chains. Thus the deduced structure is a three-dimensional network bridged by the dicarboxylate ligands and halide ions, as shown in Fig. 10b.

The ruthenium(II,III) dicarboxylates **10–12** have displayed the ability to adsorb a large amount of gas. The maximum amounts of nitrogen, oxygen, and argon adsorbed are summarized in Table 6. The maximum amount increases in the order: **10** < **11** < **12**. The gas adsorption properties depend upon the diameter of the capillary, which is controlled by the size and structure of the dicarboxylate ligands, as was also recognized in previous studies of

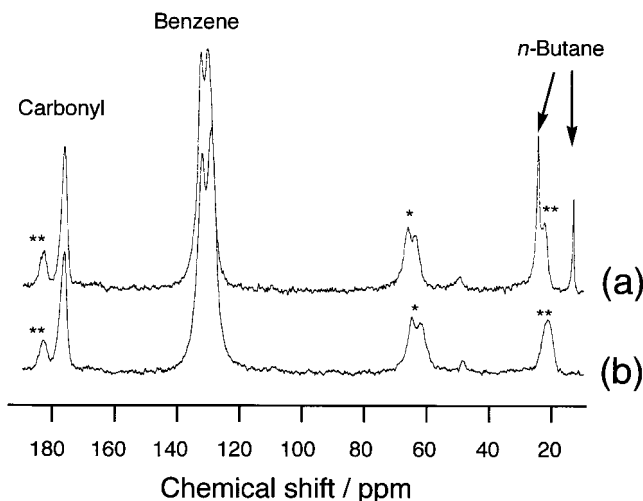


FIG. 8. ^{13}C CP/MAS NMR spectra of complex (**6**); (a) **6** with *n*-butane and (b) dried **6**. *, Springing side bands; **, bands of acetate impurity.

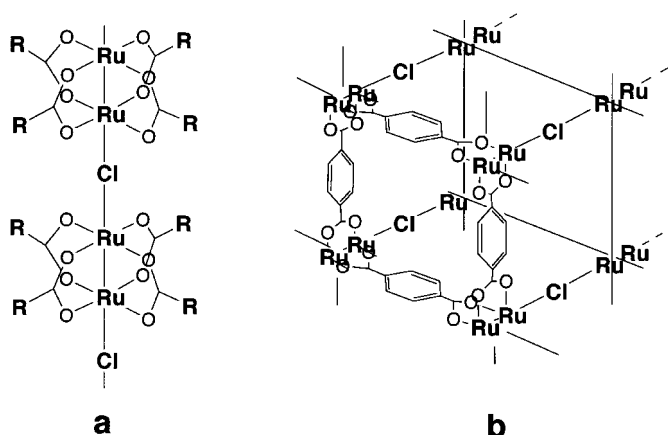
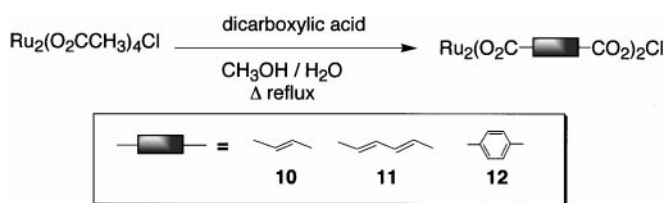


FIG. 10. Linear structure of mixed-valence ruthenium(II,III) acetate bridged by chloride (a) and three-dimensional structure of ruthenium(II,III) dicarboxylate (b).



SCHEME 3

copper(II) and molybdenum(II) dicarboxylates. This result suggests that complexes **10–12** would form a capillary structure similar to that of copper(II) dicarboxylates and molybdenum(II) dicarboxylates.

2.2. Dinuclear Transition-Metal Carboxylates Bridged by Ligands in the Axial Direction

The building blocks bearing noncovalent interaction sites can form network structure. Such interactions build and stabilize the micropore structure occluding gases.

All of the metal dicarboxylates described in the previous sections have two- or three-dimensional network structures. We found that the microporous structure constructed also by self-assembly of infinite linear chain complexes, transition-metal benzoates, and substituted benzoate bridged by pyrazine ($\text{M}_2(\text{O}_2\text{CC}_6\text{H}_5)_4(\text{pyz})$). The van der Waals interaction between phenyl groups of ligands, so called π - π stack, may act as driving force for the self-assembly of the one-dimensional complexes.

Rhodium(II) complexes (30). Rhodium(II) benzoate and substituted benzoates are synthesized by the ligand exchange reaction between rhodium(II) acetate and corresponding carboxylic acids in diglym at 180°C. (Scheme 4) Rhodium(II) carboxylates bridged by pyrazine are quantitatively yielded as yellowish-brown microcrystals. Heating the microcrystals for 2 h at 100°C in vacuum produced

TABLE 5
Raman and For-IR Spectra and Effective Magnetic Moments (μ_{eff}) of Ruthenium(II,III) Dicarboxylates **10–12**

Complex	Raman $\nu(\text{Ru-Ru})/\text{cm}^{-1}$	Far IR		$\mu_{\text{eff}}^a/\text{BM}$ (at rt)
		$\nu(\text{Ru-Cl})/\text{cm}^{-1}$	$\nu(\text{Ru-O})/\text{cm}^{-1}$	
$\text{Ru}_2(\text{O}_2\text{CCH}_3)_4\text{Cl}$	326 ^b	340 ^c	403 ^c	4.16 ^d
10	334	340	410	3.75
11	336	325	364m, 485m	3.78
12	336	334	385s, 411w	4.04

^aGouy method

^bRef. 29a.

^cRef. 29b.

^dMeasured by carrying magnetometer for complexes.

TABLE 6

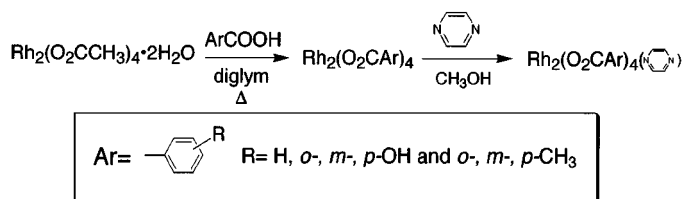
Amounts of Adsorbed Gases in Ruthenium(II) Dicarboxylates **10–12**

Complex		Amount of occlusion (mol/mol of Ru atoms)		
		N ₂	O ₂	Ar
$\text{Ru}_2(\text{OOC}-\text{[ligand]}-\text{COO})_2\text{Cl}$	10	0.7	1.0	0.8
$\text{Ru}_2(\text{OOC}-\text{[ligand]}-\text{COO})_2\text{Cl}$	11	1.1	1.4	1.2
$\text{Ru}_2(\text{OOC}-\text{[ligand]}-\text{COO})_2\text{Cl}$	12	1.3	1.7	1.4

yellowish-brown microcrystals, which are capable of occluding gases. The maximum amounts of adsorbed N₂ gas for the rhodium(II) complexes are summarized in Table 7. The maximum amount of adsorbed gas for rhodium(II) benzoate-pyrazine is almost equal to that for copper(II) terephthalate (**2**). The magnetic susceptibilities were measured by the Gouy method at room temperature. The effective magnetic moments (μ_{eff}) of the rhodium(II) complexes are almost equal to those for dinuclear rhodium(II) carboxylates, such as rhodium(II) acetate, indicating the existence of the same dinuclear structure in the present rhodium(II) carboxylates which have pyrazine bridges, forming the one-dimensional structure shown in Fig. 11a. The one-dimensional polymer complex is the elementary component used to construct the micropores in which a large amount of gases can be occluded.

The three-dimensional structure, which has a large micropores, as shown in Fig. 11b, is a reasonable proposal for our rhodium(II) carboxylates-pyrazine by analogy with the structure of copper(II) terephthalate (**2**), which shows adsorption behavior that is similar to the rhodium(II) salt. We determined the crystal structure of the microporous copper(II) benzoate-pyridine (**31**) that constructs micropores as shown in Fig. 11b.

The TG-DTA curves, shown in Fig. 12, clearly indicate the thermal stability of rhodium(II). There is neither any endo- nor any exothermic peak nor is there any remarkable weight loss at temperatures below 520 K (thermal



SCHEME 4

TABLE 7

Compound	μ_{eff} (BM/Rh at rt)	Amount of occlusion (mol/mol of rhodium atoms)
$\text{Rh}_2(\text{O}_2\text{C}-\text{C}_6\text{H}_4-\text{R})_4(\text{N}_4)$		
$R = \begin{cases} \text{H} \\ o\text{-OH} \\ m\text{-OH} \\ p\text{-OH} \\ o\text{-CH}_3 \\ m\text{-CH}_3 \\ p\text{-CH}_3 \end{cases}$	$\begin{cases} 0.38 \\ 0.27 \\ 0.21 \\ 0.30 \\ 0.25 \\ 0.33 \\ 0.19 \end{cases}$	$\begin{cases} 1.8 \\ 1.1 \\ 0.8 \\ 0.6 \\ 0.2 \\ 0.5 \\ 0.6 \end{cases}$

decomposition temperature, 540–600 K). It is noteworthy that the micropores of the rhodium(II) carboxylates–pyrazine are surprisingly thermally stable, although the micropores are formed from one-dimensional polymer complexes with weak van der Waals force between phenyl groups (32).

3. OUTLOOK AND REMARKS

The noncovalent bond networks whose structures are constructed through inter- and/or intramolecular interaction are frequently seen in the biological systems (33). Aoyama (34) reported that self-assembly of organic molecules such as anthracene and porphyrin derivatives forms a hydrogen-bonded network together with a variety of guest molecules in their cavities. Tadokoro (35) reported a unique

transition-metal complex 3D system building block, metal tris(biimidazolato) complex, in which each of the three π -conjugated biimidazolato ligands provide an intermolecular $\text{NH} \cdots \text{N}$ -type hydrogen-bonding site. The complexes organized to form alternative 2D structures.

The 3D networks frequently interpenetrate them in the solid state. Inorganic interpenetrating 3D system was reviewed by Batten (36). Fujita (37) and Kitagawa (38) each developed the area of the design of metal bipyridine complex with an open framework. Yaghi (19,39) synthesized zinc(II) polycarboxylate system with an open framework. In the chemistry of complexes, porous complexes are known as a thermally unstable. Their porous structures are only stable with crystal molecules and/or counter ions in their micropores. The generation of microporous transition-metal complexes with thermal stability (stable micropore structure under even drying condition) is of great interest.

Since 1995, after we had applied to patent adsorbent microporous complexes (40), we have continued to study adsorbent microporous complexes. There are many excellent works of adsorbent porous complexes reported by Yaghi (12, 41), Kitagawa (42), and Williams (43).

4. FUTURE PROSPECTS

Complex chemistry consists of the characteristics of transition metals (inorganic species) and organic ligands (organic species). Considering the distinguishable features of inorganic compounds and organic compounds, the network

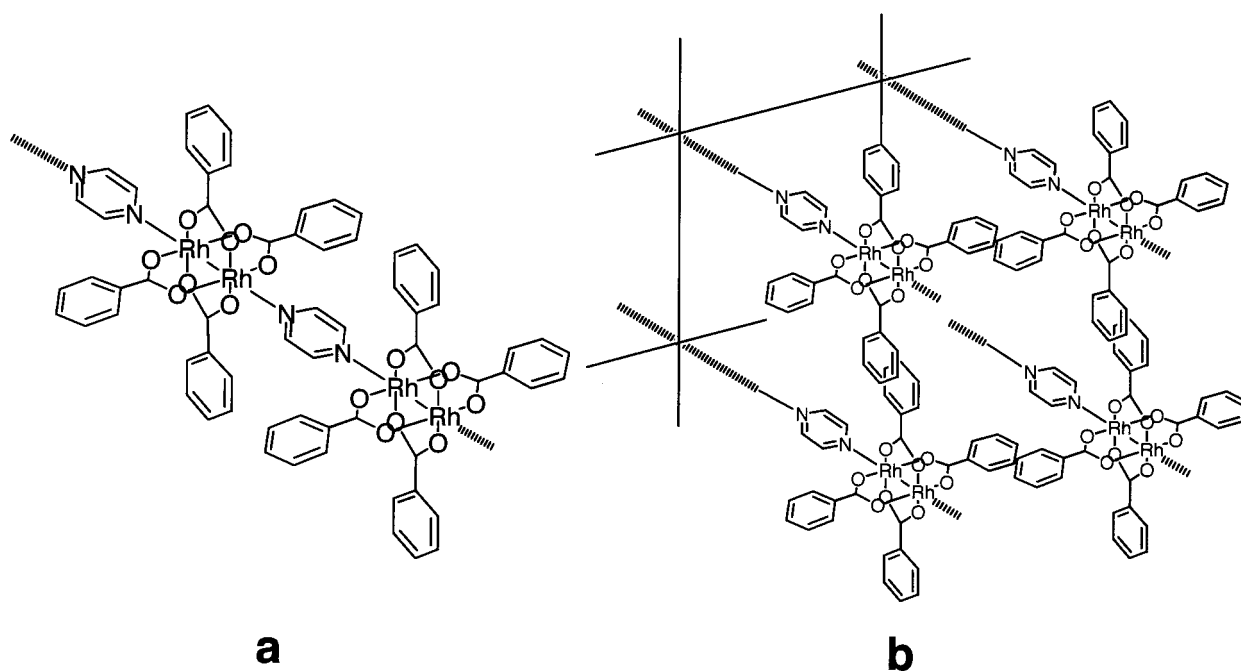


FIG. 11. Linear structure of rhodium(II) benzoate–pyrazine (a) and proposed porous structure in crystalline state (b).

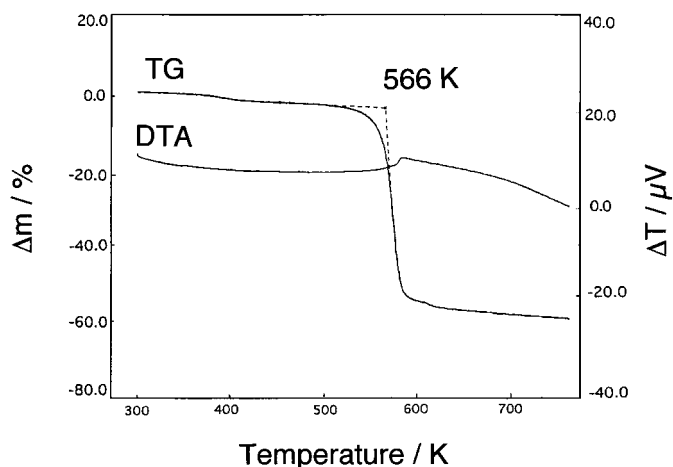


FIG. 12. TG-DTA curves of rhodium(II) benzoate-pyrazine.

structure containing transition-metal complexes is expected to have a wide range of features from organic to inorganic. Three-dimensional network structures containing transition metal complexes would display cooperative and/or emphasized properties due to the softness of the transition-metal complexes, whose properties are embellished by the selection of metal and ligands.

The possibilities of long-range organometallic conjugation is of great interest due to the ability of constructing purpose-oriented materials with useful properties, for example electronic, magnetic, optical, and catalytic materials derived from long-range $p\pi-d\pi$ and/or $d\pi-d\pi$ interaction (44). The following applications are among those considered: pooling gas, molecular sieves, molecular recognition, gas phase catalysis (45), building specific surfaces, hybrid materials (46), the field which manifests the new physical property of the adsorbed molecule (47), the material of the quantum chemistry (48), etc. Microporous inorganic compounds such as zeolites have the ability to adsorb molecules, exchange ions, and heterogeneously catalyze. Thus existing microporous transition-metal complexes will provide functional substances combined with novel physical properties including optic, electronic, and magnetic properties (49).

ACKNOWLEDGMENT

The authors thank Professors K. Yamaguchi and A. Nakamura for their helpful discussions. The authors also thank Professor M. Mikuriya for his kind collaboration, Professor S. Takeda for providing solid-state NMR measurement, and Dr. K. Seki for providing isotherm measurement. This work was supported by Grant-in-Aids for Specially Promoted Research (Grant 06101004, A. Nakamura) and Scientific Research Grants 10149253 and 10554041 from the Ministry of Education, Science, Sports, and Culture of Japan. Finally we are indebted to Professor O. M. Yaghi for his invitation to contribute to this special issue.

REFERENCES

- (a) A. F. Constedt, *Akad. Hantle. Stochholm* **18**, 120 (1756); (b) A. Damour, *Ann. Mines* **17**, 191 (1840).
- (a) R. K. Iler, "The Chemistry of Silica, Wiley, New York, 1979; R. Szostack, *Molecular Sieves*," 2nd ed., Blackie Academic and Professional, London, 1998; (b) L. L. Henchi and D. R. Ulrich, *Ultrastructure Processing of Ceramics, Glasses, and Composites*, Wiley, New York, 1984; (c) R. E. Grin, "Applied Clay Mineralogy," McGraw-Hill, New York 1962; (d) R. F. Lobo *et al.* (Eds.), *Microporous and Macroporous Materials*, Materials Research Society, Pittsburgh, 1996.
- M. Kato, H. B. Jonassen, and J. C. Fanning, *Chem. Rev.* **6**, 99 (1964).
- J. N. van Niekerk and F. R. L. Schoening, *Acta Crystallogr.* **6**, 227 (1953).
- (a) W. Mori, F. Inoue, K. Yoshida, H. Nakayama, S. Takamizawa, and M. Kishita, *Chem. Lett.* **1997**, 1219 (1997); (b) W. Mori and S. Takamizawa, *Kagaku to Kogyo* **51**, 210 (1998). [Japanese]
- B. Bleaney and K. D. Bowers, *Proc. R. Soc. London A* **214**, 415 (1971).
- O. Kahn, "Molecular magnetism," VCH, Weinheim, 1993.
- (a) B. N. Figgis and R. L. Martin, *J. Chem. Soc.* 3937 (1956); (b) A. K. Gregson, R. L. Martin, and S. Mitra, *Proc. R. Soc. London A* **320**, 473 (1971).
- (a) O. Asai, M. Kishita, and M. Kubo, *Naturwissenschaften* **46**, 1 (1959); (b) O. Asai, M. Kishita, and M. Kubo, *J. Phys. Chem.* **63**, 96 (1959).
- G. Horvath and K. Kawazoe, *J. Chem. Eng. Jpn.* **6**, 470 (1983).
- S. J. Gregg and K. S. W. Sing, "Adsorption, Surface Area, and Porosity," 1st ed., Chap. 1, Academic Press, New York, 1967.
- H. Li, M. Eddaoudi, T. L. Groy, and O. M. Yaghi, *J. Am. Chem. Soc.* **120**, 8571 (1998).
- (a) F. A. Cotton, C. E. Rice, G. W. Rice, *J. Am. Chem. Soc.* **99**, 4704 (1977); (b) F. A. Cotton and G. W. Rice, *Inorg. Chem.* **17**, 2004 (1978).
- (a) F. A. Cotton, L. M. Daniel, P. A. Kibala, M. Matusu, W. J. Roth, W. Shwotzer, W. Wang, and B. Zhong, *Inorg. Chim. Acta* **215**, 9 (1994); (b) D. S. Martin and H.-W. Hueng, *Inorg. Chem.* **29**, 3674 (1990); (c) F. A. Cotton, Z. C. Mester, T. R. Webb, *Acta Crystallogr. B* **30**, 2768 (1974).
- (a) D. V. Baxter, R. H. Cayton, M. H. Chisholm, J. C. Huffman, E. F. Putilina, S. L. Tagg, J. L. Wesemann, J. W. Zwanziger, and F. D. Darrington, *J. Am. Chem. Soc.* **116**, 4551 (1994); (b) M. H. Chisholm, H. T. Chiu, and J. C. Huffman, *Polyhedron* **3**, 759 (1984).
- (a) M. J. Benett, W. K. Bratton, F. A. Cotton, and W. R. Robinson, *Inorg. Chem.* **7**, 1570 (1968); (b) D. M. Collins, F. A. Cotton, and L. D. Gage, *Inorg. Chem.* **18**, 1712 (1979).
- (a) R. W. Mitchell, A. Spencer, and G. Wilkinson, *J. Chem. Soc. Dalton Trans.* 846 (1973); (b) M. H. Chisholm, G. Christon, K. Foltling, J. C. Huffman, C. A. James, J. A. Sanuels, J. L. Wesemann, and W. H. Woodruff, *Inorg. Chem.* **35**, 3643 (1996).
- F. A. Cotton and R. A. Walton, "Multiple Bonds between Metal Atoms," 2nd ed., Oxford Univ. Press, New York, 1993, and Refs. therein.
- H. Tamura, K. Ogawa, and W. Mori, *J. Crystallogr. Spectrosc. Res.* **19**(1), 203 (1989).
- W. Mori *et al.*, submitted for publication.
- S. Takamizawa, W. Mori, M. Furihata, S. Takeda, and K. Yamaguchi, *Inorg. Chim. Acta* **283**, 268 (1998).
- T. A. Stephenson, E. Bannister, G. Wilkinson, *J. Chem. Soc.* 2538 (1964).
- W. K. Bratton *et al.*, *J. Coord. Chem.* **1**, 121 (1971).
- J. A. Barth, *Z. Anorg. Allg. Chem.* **398**, 2538 (1973).
- (a) S. Takamizawa, K. Yamaguchi, and W. Mori, *Inorg. Chem. Commun.* **1**, 177 (1998); (b) S. Takamizawa, T. Ohmura, K. Yamaguchi, and W. Mori, *Mol. Cryst. Liq. Cryst.*, in press.
- M. Yamashita, K. Inoue, T. Ohishi, T. Takeuchi, T. Yoshida, and W. Mori, *Mol. Cryst. Liq. Cryst.*, *fl2* **274**, 25 (1995).

27. J. G. Norman, G. E. Renzoni, and D. A. Case, *J. Am. Chem. Soc.* **101**, 5256 (1979).
28. R. J. H. Clark and L. T. H. Ferris, *Inorg. Chem.* **20**, 2759 (1981).
29. (a) T. A. Stephenson and G. Wilkinson, *J. Inorg. Nucl. Chem.* **28**, 2285 (1966); (b) M. Mukaida, T. Nomura, and T. Ishimori, *Bull. Chem. Soc. Jpn.* **45**, 2143 (1972).
30. (a) W. Mori, H. Hoshino, Y. Nishimoto, and S. Takamizawa, *Chem. Lett.* **331** (1999); (b) W. Mori, H. Hoshino, K. Horikawa, Y. Nishimoto, and S. Takamizawa, *Mol. Cryst. Liq. Cryst.*, in press.
31. R. Nukada, W. Mori, S. Takamizawa, M. Mikuriya, M. Handa, and H. Naono, *Chem. Lett.* 367 (1999).
32. C. A. Hunter and J. K. M. Sanders, *J. Am. Chem. Soc.* **112**, 5525 (1990).
33. (a) G. A. Jeffery and W. Saenger, "Hydrogen Bonding in Biological Structures," Springer, Berlin, 1991; (b) G. A. Jeffery, "An Introduction to Hydrogen Bonding," Oxford Univ. Press, New York, 1997.
34. (a) Y. Aoyama, K. Endo, T. Anzai, Y. Yamaguchi, T. Sawaki, K. Kobayashi, N. Kanehisa, H. Hashimoto, Y. Kai, and H. Masuda, *J. Am. Chem. Soc.* **118**, 5562 (1996); (b) K. Endo, T. Sawaki, M. Koyanagi, K. Kobayashi, H. Masuda, and Y. Aoyama, *J. Am. Chem. Soc.* **117**, 8341 (1995); (c) K. Kobayashi, M. Koyanagi, K. Endo, H. Masuda, and Y. Aoyama, *Chem. Eur. J.* **4**, 417 (1998).
35. M. Tadokoro, K. Isobe, H. Uekusa, Y. Ohashi, J. Toyoda, K. Tashiro, and K. Nakasuji, *Angew. Chem. Int. Ed.* **38**, 95 (1999).
36. (a) S. R. Batten and R. Robson, *Angew. Chem. Int. Ed.* **37**, 1460 (1998); (b) A. F. Wells, "Three-Dimensional Nets and Polyhedra," Wiley Interscience, New York, 1977.
37. (a) M. Fujita, J. Yazaki, and K. Ogura, *J. Am. Chem. Soc.* **112**, 5645 (1990); (b) M. Fujita, O. Sasaki, T. Mitsuhashi, T. Fujita, J. Yazaki, K. Yamaguchi, and K. Ogura, *Chem. Commun.* 1535 (1996); (c) M. Fujita, F. Ibukuro, H. Hagihara, and K. Ogura, *Nature* **367**, 720 (1994); (d) M. Aoyagi, K. Biradha, and M. Fujita, *J. Am. Chem. Soc.* **121**, 7457 (1999); (e) M. Fujita, N. Fujita, K. Ogura, and K. Yamaguchi, *Nature* **400**, 52 (1999).
38. S. Kitagawa and M. Kondo, *Bull. Chem. Soc. Jpn.* **71**, 1739 (1998).
39. (a) O. M. Yaghi, G. Li, and H. Li, *Nature* **378**(14), 703 (1995); (b) O. M. Yaghi, C. E. Davis, G. Li, and H. Li, *J. Am. Chem. Soc.* **119**, 2861 (1997); (c) O. M. Yaghi, *Acc. Chem. Res.* **31**, 474 (1998).
40. W. Mori, S. Takamizawa, M. ujiwara, and K. Seki, Patent JP 09132580 (1995) and EP 0727608 (1996).
41. (a) T. M. Reineke, M. Eddaoudi, M. Fehr, D. Kelley, and O. M. Yaghi, *J. Am. Chem. Soc.* **121**, 1651 (1999); (b) H. Li, M. Eddaoudi, M. O'Keeffe, and O. M. Yaghi, *Nature* **42**, 276 (1999).
42. M. Kondo, T. Yoshitomi, K. Seki, H. Matsuzaka, and S. Kitagawa, *Angew. Chem. Int. Ed. Engl.* **36**, 1725 (1997).
43. S.-Y. Chui, S. M.-F. Lo, J. P. H. Charmant, A. G. Orpen, and I. D. Williams, *Science* **283**, 148 (1999).
44. (a) A. Nakamura, *Bull. Chem. Soc. Jpn.* **68**, 1515 (1995); (b) M. Nishino, S. Takamizawa, Y. Kitagawa, Y. Takano, T. Onishi, H. Nagao, Y. Yoshioka, K. Mashima, A. Nakamura, and K. Yamaguchi, *Bull. Chem. Soc. Jpn.* submitted.
45. W. Mori and S. Takamizawa, *Catal. Catal.* **42**(1), 40 (2000). [Japanese]
46. (a) S. Takamizawa, M. Furihata, S. Takeda, K. Yamaguchi, and W. Mori, *Polym. Adv. Technol.*, in press; (b) S. Takamizawa, *Kagaku to Kogyo* **53**, 136 (1998). [Japanese]
47. W. Mori, T. C. Kobayashi, J. Kurobe, K. Amaya, Y. Narumi, T. Kumada, K. Kindo, H. A. Katori, T. Goto, N. Miura, S. Takamizawa, H. Nakayama, and K. Yamaguchi, *Mol. Cryst. Liq. Cryst.* **306**, 1 (1997).
48. (a) T. Kawakami, S. Takamizawa, Y. Kitagawa, W. Mori, K. Yamaguchi, and K. Katsumata, *Mol. Cryst. Liq. Cryst.*, in press; (b) S. Takamizawa, W. Mori, Y. Yokomichi, Y. Kitagawa, T. Maruta, T. Kawakami, Y. Yoshioka, and K. Yamaguchi, *Mol. Cryst. Liq. Cryst.*, in press.
49. (a) K. Yamaguchi, S. Takamizawa, Y. Kitagawa, T. Onishi, H. Nagao, Y. Yoshioka, T. Okamura, and N. Ueyama, *J. Chem. Phys.*, submitted; (b) H. Nagao, Y. Kitagawa, T. Onishi, Y. Shigeta, S. Takamizawa, Y. Yoshioka, and K. Yamaguchi, *J. Chem. Phys.*, submitted.